

14. Wharam, D. A. *et al.* One-dimensional transport and the quantisation of the ballistic resistance. *J. Phys. C* **21**, L209–L214 (1988).
15. Cowley, J. M. in *Diffraction Physics* 62–63 (Elsevier, Amsterdam, 1975).
16. Kondo, Y. & Takayanagi, K. Gold nanobridge stabilized by surface structure. *Phys. Rev. Lett.* **79**, 3455–3458 (1997).
17. Maxwell, J. C. in *A Treatise on Electricity and Magnetism* (Clarendon, Oxford, 1904).
18. Sharvin, Y. V. A possible method for studying fermi surfaces. *Sov. Phys. JETP* **21**, 655–656 (1965).
19. Landauer, R. Spatial variation of currents and fields due to localized scatterers in metallic conduction. *IBM J. Res. Dev.* **1**, 223–231 (1957).
20. Kubo, R. Statistical-mechanical theory of irreversible process. I. General theory and simple applications to magnetic and conduction problems. *J. Phys. Soc. Jpn* **12**, 570–586 (1957).
21. Landman, U., Luedtke, W. D., Burnham, N. A. & Colton, R. J. Atomic mechanics and dynamics of adhesion, nanoindentation, and fracture. *Science* **248**, 454–461 (1990).
22. Bratkovsky, A. M., Sutton, A. P. & Todorov, T. N. Conditions for conductance quantization in realistic models of atomic-scale metallic contacts. *Phys. Rev. B* **52**, 5036–5051 (1995).
23. Sørensen, M. R., Brandbyge, M. & Jacobsen, K. W. Mechanical deformation of atomic-scale metallic contacts: structure and mechanisms. *Phys. Rev. B* **57**, 3283–3294 (1998).

Correspondence and requests for materials should be addressed to H.O. (e-mail: ohnishi@tapro.jst.go.jp).

Formation and manipulation of a metallic wire of single gold atoms

A. I. Yanson*, G. Rubio Bollinger†, H. E. van den Brom*, N. Agrait† & J. M. van Ruitenbeek*

*Kamerlingh Onnes Laboratorium, Leiden University, PO Box 9504, NL-2300 RA Leiden, The Netherlands

†Laboratorio de Bajas Temperaturas, Dept Física de la Materia Condensada C-III, Instituto Universitario de Ciencia de Materiales “Nicolás Cabrera”, Universidad Autónoma de Madrid, E-28049 Madrid, Spain

The continuing miniaturization of microelectronics raises the prospect of nanometre-scale devices with mechanical and electrical properties that are qualitatively different from those at larger dimensions. The investigation of these properties, and particularly the increasing influence of quantum effects on electron transport, has therefore attracted much interest. Quantum properties of the conductance can be observed when ‘breaking’ a metallic contact: as two metal electrodes in contact with each other are slowly retracted, the contact area undergoes structural rearrangements until it consists in its final stages of only a few bridging atoms^{1–3}. Just before the abrupt transition to tunnelling occurs, the electrical conductance through a monovalent metal contact is always close to a value of $2e^2/h$ ($\approx 12.9 \text{ k}\Omega^{-1}$), where e is the charge on an electron and h is Planck’s constant^{4–6}. This value corresponds to one quantum unit of conductance, thus indicating that the ‘neck’ of the contact consists of a single atom⁷. In contrast to previous observations of only single-atom necks, here we describe the breaking of atomic-scale gold contacts, which leads to the formation of gold chains one atom thick and at least four atoms long. Once we start to pull out a chain, the conductance never exceeds $2e^2/h$, confirming that it acts as a one-dimensional quantized nanowire. Given their high stability and the ability to support ballistic electron transport, these structures seem well suited for the investigation of atomic-scale electronics.

The experimental techniques used for studies on metallic contacts of atomic dimensions are all based on piezoelectric transducers which allow fine positioning of two metal electrodes with respect to each other. Scanning tunnelling microscopy (STM), in which the tip is driven into contact with a metal surface and the conductance is measured during subsequent retraction, has been widely used for this purpose^{4,5,8,9}. The other commonly used technique employs a mechanically controllable break-junction (MCB). In this case, one starts with a macroscopic notched wire¹⁰, or a nanofabricated metal bridge¹¹ mounted on a flexible substrate. The wire (or bridge) is broken at low temperatures in vacuum, and contact is re-established between the fracture surfaces by piezoelectric control of substrate

bending. Here we have used both MCB and a very stable STM at liquid-helium temperatures to produce and study chains of single gold atoms. In each case, high-purity (>99.99%) gold was used. Conductance was measured at a 10 mV d.c. voltage bias with 1% accuracy.

An example of a conductance curve obtained while stretching a gold nanocontact in an MCB is presented in Fig. 1. The curve reflects the evolution of some particular atomic configuration, during which the conductance decreases in a series of sharp vertically descending steps, with a gradual slope on the plateaux in between. These steps have been shown to be the result of atomic structural rearrangements^{9,12}. The curves for successive rupture sequences do not repeat in detail, as they depend on the exact atomic positions in the contact. However, many curves have one striking feature in common: the remarkable length of the last conductance plateau just before rupture, at the value of about one conductance quantum, $G_0 = 2e^2/h$. Previous experiments have shown that the conductance at the last plateau for monovalent metals is usually close to $1 G_0$ (refs 4–6), and it has been argued that these plateaux correspond to a contact with a single atom at the narrowest cross-section⁷. Examples have been found previously of exceptionally long stretched last plateaux, in particular for gold (see, for example, ref. 20), but this has not received due attention. The interest becomes clear when we recognize that the conductance of a point contact is determined predominantly by the size of its narrowest cross-section and that, during contact elongation, all structural transformations are localized to the neck region^{2,3,12}. Figure 1 shows that during the last stage of elongation the conductance stays in a limited range of values corresponding to one atom in cross-section, while the contact is being stretched over distances up to 20 Å. This suggests the possibility that the contact stretches to form a chain of single atoms. As we cannot image the

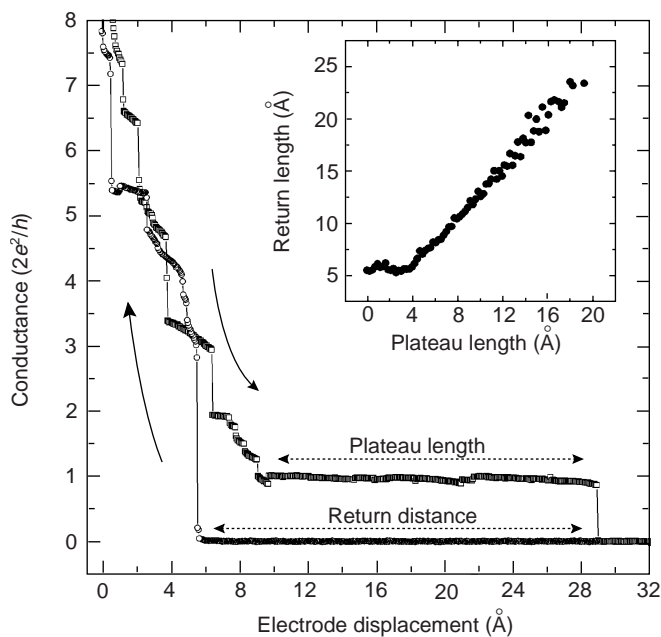


Figure 1 Conductance as a function of the displacement of the two gold electrodes with respect to each other in an MCB experiment at 4.2 K. The trace starts at the upper left, coming from higher conductance values (open squares). A long plateau with a conductance near $1 G_0$ is observed and, after a jump to tunnelling, the electrode needs to return by a little more than the length of the long plateau to come back into contact (open circles). Inset, the average of the return distance as a function of the length of the long plateau (recorded with an STM at 4.2 K). The relation is approximately 1:1, with an offset of 5 Å which is probably due to the elasticity of the atomic structure.

atomic structure of the neck directly, we performed the following experiments in order to test this hypothesis.

Figure 1 illustrates that the distance the electrode needs to travel back to re-establish contact after rupture is almost equal to the length of the last plateau itself. We have recorded these lengths for a large number of contacts, and the average return distance is plotted in Fig. 1 inset as a function of the length of the last plateau. The relation is approximately 1:1, suggesting that a fragile structure is formed with a length corresponding to that of the last plateau, which is unable to support itself when it breaks and collapses onto the 'banks' on either side.

The probability distribution for pulling a long last plateau as a function of its length was obtained by recording a histogram of plateau lengths (Fig. 2). Instead of a smooth distribution, we find a series of three equidistant peaks, with a shoulder at the fourth and fifth position. The probability of pulling a structure of length L decreases rapidly for large L and drops below 10^{-4} for $L > 20 \text{ \AA}$, so the longest observed plateaux have a length of 25 \AA . The shape of the histogram suggests that the nanobridges tend to be elongated by integer multiples of 3.6 \AA , which is somewhat longer than the nearest-neighbour spacing 2.88 \AA of gold atoms in the crystal.

As a further test, we carried out STM experiments during which one of the electrodes was moved laterally once a plateau of a given length was formed. For a short length of the last plateau (Fig. 3a), when we start oscillating the STM tip sideways (Fig. 3b), we observe rupture of the contact at low oscillation amplitudes. Repeating the experiment for longer elongation of the last plateau (Fig. 3c), fracture is observed at much larger lateral displacement amplitudes (Fig. 3d) and the bridge is found to collapse. The small jumps in the conductance in Fig. 3b and d have the same origin as those found during elongation of the last plateau in Fig. 1. That is, they are due to atomic structural rearrangements, which have only a minor effect on the conductance as long as the narrowest cross-section is still a single atom. The two atomic configurations at each side of the small conductance jump are separated by an energy barrier, which can be surmounted by applying a sufficiently large force. This force stretches the atomic bridge over a length proportional to its elasticity. Consequently, the hysteresis of the conductance jumps that occur as the structure is moved laterally (Fig. 3d) indicates that longer structures have a larger lateral elasticity than short ones.

We find that there is a significant probability for formation of a long bridge with a length given by that of the last plateau, which

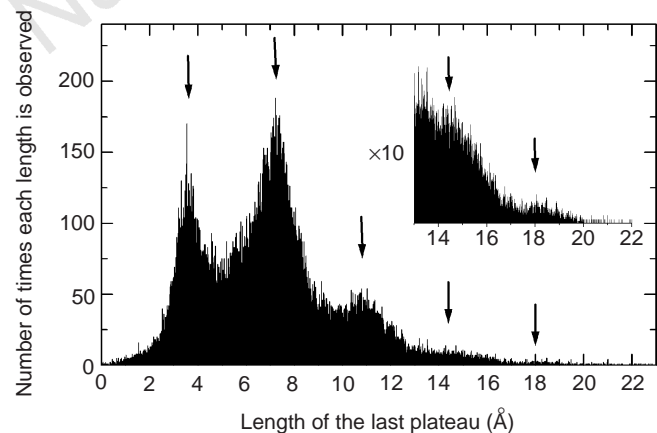


Figure 2 The distribution of lengths for the last plateau, obtained in $\sim 100,000$ experiments similar to those described in Fig. 1, shows a number of equidistant maxima. The arrows are positioned at multiples of 3.6 \AA . The data were recorded with an MCB at 4.2 K . The length of the last plateau was defined as the distance between the points at which the conductance drops below $1.2G_0$ and $0.8G_0$, respectively. Inset, the tail of the distribution on a $10\times$ expanded scale. The accuracy for the calibration of the length scale is 30%.

completely collapses on breaking. Its smallest cross-section is one atom and it breaks at multiples of $\sim 3.6 \text{ \AA}$ in length, which would correspond to a stretched Au–Au bond distance. We can swing the bridge sideways by a distance comparable to its length. We conclude that all the evidence combines to show that we are pulling, atom by atom, a freely suspended chain of single Au atoms. The peaks in the plateau length distribution shown in Fig. 2 correspond to the observation of chains containing up to 4 or 5 atoms. Although we cannot resolve the peak structure for longer plateaux, extrapolating the periodic structure suggests that the longest plateaux observed correspond to chains of seven atoms.

Despite its low probability of formation, once an atomic chain is pulled it remains very stable: some of the longest chains obtained in our experiments have been held stable for as long as 1 hour, after which we stopped the experiment. They can sustain very large current densities of up to $8 \times 10^{14} \text{ A m}^{-2}$ (currents up to 80 \mu A or a voltage up to 1 V), proving that the electron transport is ballistic, and that most of the power is dissipated in the electrodes far away from the contact. This makes the atomic chains suitable for investigation as conductors in atomic electronic circuits.

Once the conductance drops below $1 G_0$ at the beginning of chain formation, it never rises above this value. This is consistent with the

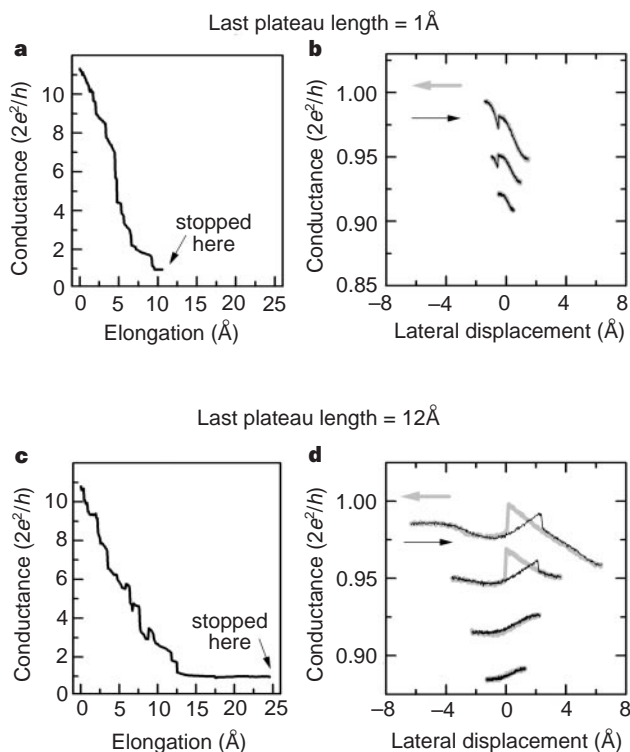


Figure 3 Swinging an atomic contact sideways by lateral displacement of one of its ends in an STM experiment. First, the elongation of the last plateau is stopped early (a), at a length of $\sim 1 \text{ \AA}$ (marked with an arrow). Then, one end of the contact is cyclically displaced perpendicular to the contact axis (b) while slowly increasing the displacement amplitude. The curves for smaller swing amplitudes are shifted by increments of $-0.03 G_0$ for clarity. The contact breaks at a lateral displacement of 1.4 \AA . Performing the same experiment for a last plateau of 12 \AA length (c) gives quite different results: rupture occurs at much larger lateral swing amplitudes of 6.3 \AA (d) and the contact bridge collapses. For small swing amplitudes the contact behaves elastically and the conductance for both directions of the swing superpose. As the amplitude is increased, small hysteric jumps in conductance take place (note the expanded scale), resulting from slight rearrangements of the atoms in the chain or at its bases.

notion of the conductance being perfectly described by one single quantum mode⁷. Fluctuations to lower values correspond to a reduced transmission probability for this mode as a result of back-scattering, but the maximum value should be limited to $1 G_0$, in agreement with the observations. In this sense, our metallic atomic wire is a perfectly quantized one-dimensional conductor. Previously, Yazdani *et al.*¹⁵ succeeded in measuring the conductance of a chain of two atoms of the noble-gas xenon, which was found to be orders of magnitude lower than the quantum unit of conductance due to the lack of metallic bonding. A recent calculation by Lang¹⁴ on single atomic chains of up to four sodium atoms predicts their conductance to fall below $0.7 G_0$, fluctuating with the chain length. This is somewhat smaller than the experimental values, which almost all fall in the range from 0.8 to $1 G_0$ (see, for example, Figs 1 and 3). This discrepancy may be influenced by the interface to the 'jellium' electrodes used in the calculation.

Recent molecular-dynamics simulations of metallic nanocontacts by Sutton and Todorov (unpublished work), Sørensen *et al.*^{15,16} and Finbow *et al.*¹⁷ support the plausibility of occasional formation of atomic chains, although these authors note that their model interatomic potential may not be reliable for these unusual one-dimensional structures. Advanced first-principles molecular-dynamics calculations have been performed for Na nanocontacts at 190 K (ref. 18), and showed no indication of chain formation. Although it is not clear to us what determines the difference in behaviour between gold and sodium, this result is consistent with the fact that we do not observe chain formation for sodium in the low-temperature experiments.

The atomic-chain structures should open many avenues of further investigations. Studying the mechanical properties of this unusual form of matter should enable stringent tests of our understanding of interatomic potentials. One might search for evidence of one-dimensional excitations, such as phonons and plasmons. Further, the electronic properties of these chains are expected to be those of a perfect one-dimensional conductor, where the electron-phonon interaction might lead to a Peierls transition. The electron-electron interaction may lead to the formation of a so-called Tomonaga-Luttinger liquid¹⁹, which replaces the familiar Fermi liquid description for bulk metals when the conductor becomes one-dimensional. □

Received 2 March; accepted 11 September 1998.

1. van Ruitenbeek, J. M. in *Mesoscopic Electron Transport* (eds Sohn, L. L., Kouwenhoven, L. P. & Schön, G.) 549–579 (NATO ASI Ser. E, Vol. 345, Kluwer Academic, Dordrecht, 1997).
2. Sutton, A. P. & Pethica, J. B. Inelastic flow processes in nanometre volumes of solids. *J. Phys.: Condens. Matter* **2**, 5317–5326 (1990).
3. Landman, U., Luedtke, W. D., Burnham, N. A. & Colton, R. J. Atomistic mechanisms and dynamics of adhesion, nanoindentation and fracture. *Science* **248**, 454–461 (1990).
4. Agraït, N., Rodrigo, J. G. & Vieira, S. Conductance steps and quantization in atomic-size contacts. *Phys. Rev. B* **47**, 12345–12348 (1993).
5. Pascual, J. I. *et al.* Quantum contact in gold nanostructures by scanning tunneling microscopy. *Phys. Rev. Lett.* **71**, 1852–1855 (1993).
6. Krans, J. M. *et al.* One-atom point contacts. *Phys. Rev. B* **48**, 14721–14724 (1993).
7. Scheer, E. *et al.* The signature of chemical valence in the electrical conduction through a single-atom contact. *Nature* **394**, 154–157 (1998).
8. Brandbyge, M. *et al.* Quantized conductance in atom-sized wires between two metals. *Phys. Rev. B* **52**, 8499–8514 (1995).
9. Rubio, G., Agraït, N. & Vieira, S. Atomic-sized metallic contacts: mechanical properties and electronic transport. *Phys. Rev. Lett.* **76**, 2302–2305 (1996).
10. Muller, C. J., van Ruitenbeek, J. M. & de Jongh, L. J. Experimental observation of the transition from weak link to tunnel junction. *Physica C* **191**, 485–504 (1992).
11. van Ruitenbeek, J. M. *et al.* Adjustable nanofabricated atom size contacts. *Rev. Sci. Instrum.* **67**, 108–111 (1996).
12. Todorov, T. N. & Sutton, A. P. Jumps in electronic conductance due to mechanical instabilities. *Phys. Rev. Lett.* **70**, 2138–2141 (1993).
13. Yazdani, A., Eigler, D. M. & Lang, N. D. Off-resonance conduction through atomic wires. *Science* **272**, 1921–1924 (1996).
14. Lang, N. D. Anomalous dependence of resistance on length in atomic wires. *Phys. Rev. Lett.* **79**, 1357–1360 (1997).
15. Brandbyge, M., Sørensen, M. R. & Jacobsen, K. W. Conductance eigenchannels in nanocontacts. *Phys. Rev. B* **56**, 14956–14959 (1997).
16. Sørensen, M. R., Brandbyge, M. & Jacobsen, K. W. Mechanical deformation of atomic-scale metallic contacts: structure and mechanism. *Phys. Rev. B* **57**, 3283–3295 (1998).
17. Finbow, G. M., Lynden-Bell, R. M. & McDonald, I. R. Atomic simulation of the stretching of nanoscale metal wires. *Mol. Phys.* **92** (N4), 705–714 (1997).
18. Barnett, R. N. & Landman, U. Cluster-derived structures and conductance fluctuations in nanowires. *Nature* **387**, 788–791 (1997).

19. Fisher, M. P. A. & Glazman, L. I. in *Mesoscopic Electron Transport* (eds Sohn, L. L., Kouwenhoven, L. P. & Schön, G.) 331–373 (NATO ASI Ser. E, Vol. 345, Kluwer Academic, Dordrecht, 1997).
20. Krans, J. M. *Size Effects in Atomic-Scale Point Contacts*. Thesis, Leiden Univ. (1996).

Acknowledgements. We thank B. Ludoph for many discussions, S. Vieira and L. J. de Jongh for discussions and continuous support, and A. P. Sutton, T. N. Todorov, M. R. Sørensen, M. Brandbyge and K. W. Jacobsen for communicating their results before publication. A.I.Y., H.E.v.d.B. and J.M.v.R. were supported by FOM; N.A. and G.R.B. were supported by the CICYT.

Correspondence and requests for materials should be addressed to J.M.v.R. (e-mail: ruitenbe@ruikol.LeidenUniv.nl).

Contribution of bedrock nitrogen to high nitrate concentrations in stream water

J. M. Holloway*, R. A. Dahlgren*, B. Hansen† & W. H. Casey*

* Department of Land, Air and Water Resources, University of California, Davis, California 95616, USA

† Department of Earth Sciences, University of Aarhus, Ny Munkegade, Building 520, DK-800 Aarhus C, Denmark

Concentrations of nitrate in stream water throughout the world are reported to be elevated relative to natural background levels. This enrichment is commonly attributed to anthropogenic activities such as atmospheric emissions¹, livestock feeding², agricultural runoff^{3,4}, timber harvesting practices⁵ and domestic/industrial effluent discharge^{4,6}. Here we show that bedrock containing appreciable concentrations of fixed nitrogen contribute a surprisingly large amount of nitrate to surface waters in certain California watersheds, to an extent that even small areas of these rocks have a profound influence on water quality. As 75% of the rocks now exposed at the Earth's surface are sedimentary in origin⁷, and as these rocks contain about 20% of the global nitrogen inventory⁸, 'geological' nitrogen may be a large and hitherto unappreciated source of nitrate to surface waters. Such a natural nitrate source may be especially significant given that nitrate contamination at very low levels can contribute to surface water eutrophication⁹, may cause infant methaemoglobinemia ('blue baby' syndrome)⁶ and has been implicated in certain cancers⁶. In addition, geological nitrogen may be a source of the 'missing' nitrogen noted in several biogeochemical studies of ecosystem nitrogen budgets¹.

The source(s) of nitrate contributing to eutrophication and periodic fish kills in downstream reservoirs of the Mokelumne River watershed in the central Sierra Nevada of California has been an enigma. We monitored water quality throughout the watershed over the past 2.5 years to identify the primary source(s) of nitrate entering the downstream reservoirs. Due to the close relationship we observed between streamwater nitrate concentrations and bedrock nitrogen concentrations, we specifically examined whether the bedrock could be a source of streamwater nitrate.

The Mokelumne River watershed covers an area of 980 km² extending from the Central Valley (50 m elevation) to the crest of the Sierra Nevada (3,300 m) (Fig. 1). The upper part of the watershed is dominated by Mesozoic granite and diorite and Tertiary volcanic mudflows while Palaeozoic and Jurassic rocks lie to the west in a belt of metasedimentary and metavolcanic lithologies flanking the Sierra Nevada¹⁰. Streamwater nitrate concentrations in the upper elevation watersheds have median values less than 2 μM (Fig. 1). Maximum values (~10 μM) occur during storm events in the late autumn–early winter, and low concentrations (<0.4 μM) are associated with the large amount of runoff (~70%) originating from the melting snowpack. In contrast, tributary streams in the lower watershed generally have elevated nitrate